

During its epicyclic motion, the star's azimuthal speed $\dot{\phi}$ must vary so that the angular momentum L_z remains constant:

$$\dot{\phi} = \frac{L_z}{R^2} = \frac{\Omega(R_g)R_g^2}{(R_g + x)^2} \approx \Omega(R_g) \left(1 - \frac{2x}{R_g} + \dots \right). \quad 3.73$$

Substituting from Equation 3.70 for x and integrating, we have

$$\phi(t) = \phi_0 + \Omega(R_g)t - \frac{1}{R_g} \frac{2\Omega}{\kappa} X \sin(\kappa t + \psi), \quad 3.74$$

where ϕ_0 is an arbitrary constant. Here, the first two terms give the guiding center motion. The third represents harmonic motion with the same frequency as the x oscillation in radius, but 90° out of phase, and larger by a factor of $2\Omega/\kappa$ (see Figure 3.9). The epicyclic motion is *retrograde*, in the opposite sense to the guiding center motion; it speeds the star up closer to the center, slowing it down when it is further out.

In two simple cases, the epicyclic frequency κ is a multiple of the angular speed Ω of the guiding center. In the gravitational field of a point mass, $\Omega(r) \propto r^{-3/2}$ and so $\kappa = \Omega$. The star's orbit is an ellipse with the attracting mass at one focus; the epicycles are twice as long in the ϕ direction as in x , rather than circular, as assumed by Ptolemy, Copernicus, and others who used epicycles to describe planetary motions. Within a sphere of uniform density, $\Omega(R)$ is constant and $\kappa = 2\Omega$. A star moves harmonically in an ellipse which is symmetric about the center, making

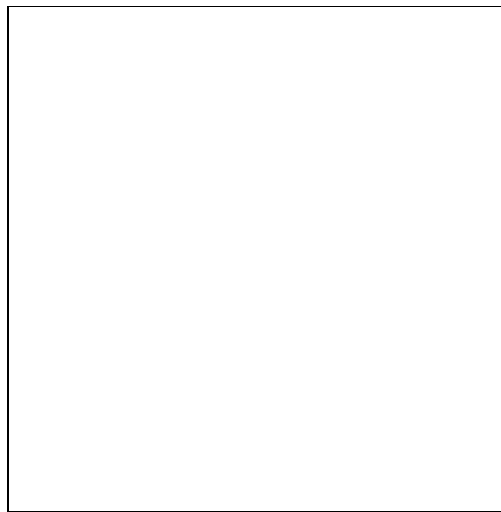


Fig. 3.10. Path of the star of Figure 3.8, viewed from above the Galactic plane; the orbit started with $(R = 1.3, \phi = 0)$ and $(\dot{R} = 0, R\dot{\phi} = 0.4574)$.

two excursions in and out during one circuit around, and the epicycles are circular. The potential of the Galaxy is intermediate between these two, so that $\Omega < \kappa < 2\Omega$. Near the Sun, $\kappa \approx 1.4\Omega$. The orbits of stars do not close on themselves; Figure 3.10 shows that they make about 1.4 oscillations in and out for every circuit of the Galaxy. We will see in Section 5.4 how stars with guiding centers at different radii R_g can be arranged on their epicycles to produce a spiral pattern in the disk.

check section number ahead

Near the Sun, the period of the epicycles is about 170 Myr, far too long for us to watch stars complete their circuits. But we can measure the velocities of stars close to us, at $R \approx R_0$. Some of these will have guiding centers further out than the Sun, and so are on the inner parts of their epicycles, while others have their guiding centers at smaller radii. Because of its epicyclic motion, a nearby star with its guiding center at $R_g > R_0$ moves *faster* in the tangential direction than a circular orbit at our radius. Equation 3.73 gives its relative speed v_y as

$$v_y = R_0[\dot{\phi} - \Omega(R_0)] \approx R_0 \left[\Omega(R_g) - 2x \frac{\Omega(R_g)}{R_g} - \Omega(R_0) \right]. \quad 3.75$$

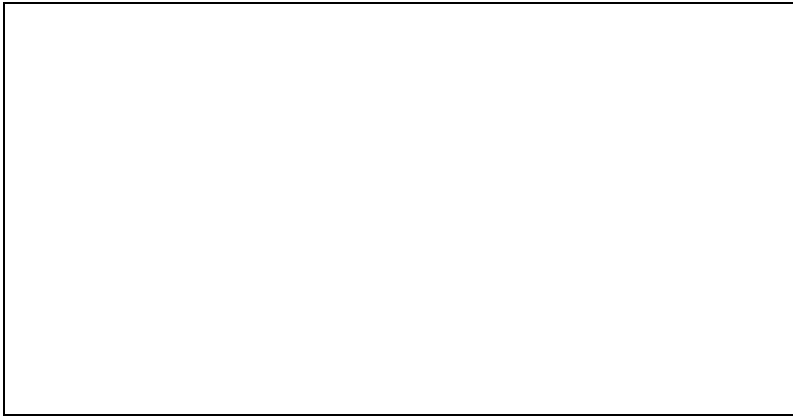


Fig. 3.11. The dispersion in velocities v_x and v_y for F and G dwarfs near the Sun increases with age. The youngest stars show a *vertex deviation*: v_x and v_y tend to have the same sign. Those stars have not yet had time to move away from the groups in which they were born. The average value of v_y is increasingly negative for older stars with larger random speeds. Open circles show stars with less than 1/4 of the Sun's iron abundance – B. Nordström et al. 2004 AAp 418, 98.

Recalling that $R_0 = R_g + x$, and dropping terms in x^2 , we have

$$v_y \approx -x \left[2\Omega(R_0) + R_0 \left(\frac{d\Omega}{dR} \right)_{R_0} \right] = -\frac{\kappa^2 x}{2\Omega} \quad \text{or} \quad 2Bx. \quad 3.76$$

We do not know the value of x for any particular star, so we take an average over all the stars we see:

$$\langle v_y^2 \rangle = \left(\frac{\kappa^2}{2\Omega} \right)^2 \langle x^2 \rangle = \frac{\kappa^2}{4\Omega^2} \langle v_x^2 \rangle. \quad 3.77$$

Since $\kappa < 2\Omega$, $\langle v_y^2 \rangle < \langle v_x^2 \rangle$; even though the epicycles are longer in the tangential y direction, the nearby stars have larger random speeds in the radial x direction. The tangential velocity dispersion is reduced because the epicycles of stars that come from further out in the Galaxy are carrying them in the same direction as the Galactic rotation, augmenting the slower motion of their guiding centers. Conversely, the epicyclic motion of stars visiting from smaller radii opposes their faster guiding center motion. For the ‘thin disk’ F and G stars of Table 2.1, we have

$$2 \lesssim \langle v_x^2 \rangle / \langle v_y^2 \rangle \lesssim 3; \quad 3.78$$

Measuring this ratio for larger groups of nearby stars provides our best estimate of the constant B ; it is about $-12 \text{ km s}^{-1} \text{ kpc}^{-1}$.

Problem 3.21: Use the result of Problem 2.17 to show that

$$\langle v_y^2 \rangle = \frac{-B}{A - B} \langle v_x^2 \rangle,$$

so that for a flat rotation curve we expect $\langle v_x^2 \rangle / \langle v_y^2 \rangle = 2$. Large studies give this ratio as 2.2; if $A = 14.8 \pm 0.8 \text{ km s}^{-1} \text{ kpc}^{-1}$, what is B ? •

The observant reader will have noticed that, in averaging, we did not take account of any radial variations in the density of stars. In fact, the stellar density is higher in the inner Galaxy, so that near the Sun we see more stars with guiding centers at smaller radii than stars that visit us from the outer Galaxy. The majority of stars will be on the outer parts of their epicycles, with $x > 0$; so according to Equation 3.76, the average tangential motion of stars near the Sun should fall behind the circular velocity. This prediction is borne out in Figure 3.11 and Table 2.1; the average $\langle v_y \rangle$ is negative, an effect known as *asymmetric drift*. The drift is stronger for groups of older stars, with larger random speeds, since their orbits deviate further from circular motion.

Problem 3.22: Show from Equation 3.71 that within a spherical galaxy of constant density, $\kappa = 2\Omega$, and the Oort constants $A = 0$ and $B = -\Omega$. For the ‘dark halo’ potential of Equation 2.19, find $\Omega(r)$ and $\kappa(r)$. Check

that they agree at small radii with those for a uniform sphere of density $V_H^2/(4\pi G a_H^2)$, and that $\kappa \rightarrow \sqrt{2}\Omega$ as r becomes large. Plot Ω , κ , $\Omega - \kappa/2$ against radius for $0 < r < 5a_H$. Show that $\Omega - \kappa/2$ approaches zero both as $r \rightarrow 0$ and as r becomes large. •

Problem 3.23: We saw in Section 2.3 that the Sun has $v_x \approx -10 \text{ km s}^{-1}$ and $v_y \approx 5 \text{ km s}^{-1}$; why do we know that its guiding center radius $R_g > R_0$? Assuming the Milky Way's rotation curve to be roughly flat, with $V(R) = R\Omega(R) = 200 \text{ km s}^{-1}$ and $R_0 = 8 \text{ kpc}$, find κ and Oort's constant B . Use Equations 3.70 and 3.76 to show that the extent of the Sun's radial excursions is $X = 0.35 \text{ kpc}$, and $R_g \approx 8.2 \text{ kpc}$. •

3.4 The collisionless Boltzmann equation

In the last section, we looked at the orbit of an individual star in the Galaxy's gravitational field. We can also describe the stars in a galaxy as we usually describe atoms in a gas: not by following the path of each atom, but by asking about the density of atoms in a particular region, and about their average motion. For simplicity, we assume here that all the stars have the same mass m .

The *distribution function* $f(\mathbf{x}, \mathbf{v}, t)$ gives the probability density in the six-dimensional *phase space* of (\mathbf{x}, \mathbf{v}) . The average number of particles (stars or atoms) in a cube of sides $\Delta x, \Delta y, \Delta z$ centred at \mathbf{x} , that have x velocity between v_x and $v_x + \Delta v_x$, y velocity between v_y and $v_y + \Delta v_y$, and z velocity between v_z and $v_z + \Delta v_z$, is

$$f(\mathbf{x}, \mathbf{v}, t) \Delta x \Delta y \Delta z \Delta v_x \Delta v_y \Delta v_z. \quad 3.79$$

The *number density* $n(\mathbf{x}, t)$ at position \mathbf{x} is the integral over velocities

$$n(\mathbf{x}, t) \equiv \int_{-\infty}^{\infty} \int_{-\infty}^{\infty} \int_{-\infty}^{\infty} f(\mathbf{x}, \mathbf{v}, t) dv_x dv_y dv_z. \quad 3.80$$

Averages such as the mean velocity $\langle \mathbf{v}(\mathbf{x}, t) \rangle$ are also given by integrals:

$$\langle \mathbf{v}(\mathbf{x}, t) \rangle n(\mathbf{x}, t) \equiv \int_{-\infty}^{\infty} \int_{-\infty}^{\infty} \int_{-\infty}^{\infty} \mathbf{v} f(\mathbf{x}, \mathbf{v}, t) dv_x dv_y dv_z. \quad 3.81$$

We want to find equations to relate changes in the density and the distribution function, as stars move about in the Galaxy, to the gravitational potential $\Phi(\mathbf{x}, t)$. For simplicity, we look at stars moving only in one direction, x . At time t , the number of stars between x and $x + \Delta x$ in the 'box' of Figure 3.12 is $n(x, t)\Delta x$. Suppose these stars move at speed $v(x) > 0$; how does $n(x)$ change with time? After a time Δt , all the stars that are now between $x - v(x)\Delta t$ and x will have entered the box, while